Available online at www.sciencedirect.com

SciVerse ScienceDirect

Journal of the European Ceramic Society 32 (2012) 471–475

www.elsevier.com/locate/jeurceramsoc

Si_3N_4 with comparable permeability to SiC

Young-Jo Park *, In-Hyuck Song

Engineering Ceramics Research Group, Korea Institute of Materials Science, 797 Changwondaero, Changwon, Gyeongnam 641-831, Republic of Korea

Received 21 July 2011; accepted 18 September 2011
Available online 7 October 2011

Abstract

Porous sintered reaction-bonded silicon nitrides (SRBSNs) with comparable permeability to SiC were fabricated using presintered Si-additive mixture granules. By increasing the granule strength through the adjustment of the presintering conditions, the strengthened sturdiness of the granules led to an increase in the pore channel size. Porous SRBSNs with ≥60% porosity were achieved without employing a pore former due to the formation of intragranular narrow pore channels as well as intergranular wide pore channels. As the specific pore area of the developed SRBSN is nearly 26 times that of SiC with similar permeability, superior filtering efficiency for nano-sized particulate matter is expected.

Keywords: A. Shaping; A. Sintering; B. Porosity; D. Si_3N_4; E. Substrate

1. Introduction

Enhancing the efficiency of machines is seen as an important means of saving energy. Hence, the working environment of machines is becoming more severe. However, there are a limited number of ceramic filters for high-temperature applications. It is common sense that the filtration of particulate matter (PM) is crucial for the health of human beings and for the performance of machines. At present, SiC is the only option for a hot gas filters in PFBC (pressurized fluidized bed combustion) and IGCC (integrated gasification combined cycle) applications.[1,2] Cordierite and SiC are two typical DPF (diesel particulate filter) materials.[3–6] These materials meet strict requirements that allow them to survive harsh conditions such as high temperatures and high gas pressures. In addition to excellent thermomechanical properties, structural aspects should be optimized to exert the best filtering performance. That is, the filtering efficiency of PM and the permeability of a clean gas need be balanced in a trade-off relationship. Trial and error efforts have shown that the size of the pore channels in a commercial hot gas filter and a DPF must be at least 10 μm.[1,4,6] With a preferred microstructure such as a complex pore channel path and a high specific pore area provided by their rod-like grain morphology, Si_3N_4 ceramics are excellent candidates for filtering media.[7–14] However, the diameter (d_p) of the pore channels in Si_3N_4 ceramics is usually restricted to ~1 μm owing to the small grain size. Generally, the size of the pore channels running through the porous structures is determined by the size of grains. The grain size in the short direction of rod-like Si_3N_4 ceramics is only a few micrometers, whereas that of SiC and cordierite ranges from several tens to hundreds of micrometers. Given that narrow pore channels ($d_p < 1$ μm) produce a large pressure drop across Si_3N_4 filters, the widening of their pore channels to the size of those in commercial filters ($d_p \geq 10$ μm) is greatly desired. Recently, the authors suggested a new concept to enhance both the filtering efficiency and the permeability of SRBSN filters via granulation of the starting powders.[15,16] Our investigation into microstructural control was aimed at forming wide channels between the granules and narrow channels within the granules. The authors demonstrated the feasibility of this concept by realizing a dual-pore-channel structure for SRBSNs.[16] In this research, a processing routine for SRBSN filters that would allow them to match the permeability of a SiC filter was investigated. It was found that porous SRBSNs could be given better filtering efficiency that equaled the permeability of SiC.

2. Experiment

The commercially available silicon powder used in this study had a purity in excess of 98.6% (Sicomill grade 2,

* Corresponding author. Tel.: +82 55 280 3356, fax: +82 55 280 3392.
E-mail address: yjpark87@kims.re.kr (Y.-J. Park).

0955-2219/$ – see front matter © 2011 Elsevier Ltd. All rights reserved.
doi:10.1016/j.jeurceramsoc.2011.09.016

Table 1
Composition of the slurry used for spray drying.

Si	Y_2O_3	Al_2O_3	$CaCO_3$	PAA	PVA	Water
100	2.67	1.33	2.05	0.53	2.12	108.7

Vesta Ceramics, Ljungaverk, Sweden; 0.4 wt.% Fe, 0.2 wt.% Al, 0.2–1.0 wt.% O, $d_{50} = 2\,\mu m$). The following commonly adopted oxide sintering additives were used: Y_2O_3 (Grade C, H. C. Stark, Goslar, Germany; 99.99%, $d_{50} = 0.7\,\mu m$), Al_2O_3 (AKP-30, Sumitomo, Tokyo, Japan; 99.99%, $d_{50} = 0.31\,\mu m$), and $CaCO_3$ (Sigma–Aldrich, 99+% purity) as the CaO source. The total amount of sintering additives, Y_2O_3–Al_2O_3–CaO, was fixed at 3 wt.%; this amount was based on the Si_3N_4 content calculated from the perfect nitridation of Si. Polyacrylic acid (PAA; Wako, Tokyo, Japan) and polyvinyl alcohol (PVA; Junsei, Tokyo, Japan) were blended in the Si-additive mixture as a dispersant and a binder, respectively. The amounts of PAA and PVA were 0.5 wt.% and 2 wt.%, respectively, of the sum of the other solid ingredients (Table 1). Granules were fabricated by spray drying, the detailed procedure of which is available in the literature.[15] The presintering of the granules was done using a tube furnace soaking at 1200 °C for 10 min (PG1) and at 1350 °C for 10 min (PG2) under a flowing (150 ml/min) Ar

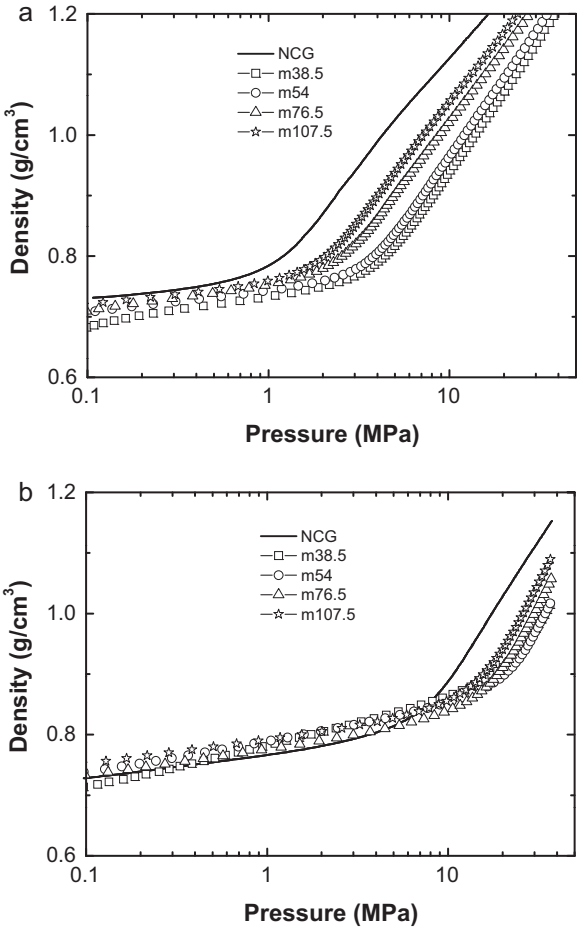

Fig. 1. Compacting behavior of presintered granules: density *vs*. pressure relationship of (a) PG1 and (b) PG2.

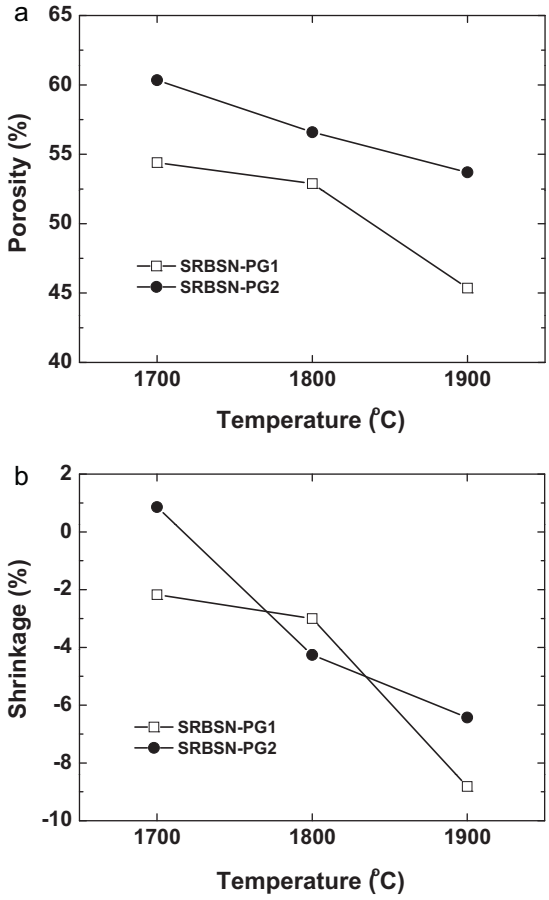

Fig. 2. Measurement of (a) the porosity and (b) the shrinkage of SRBSNs made of m76.5 granules.

atmosphere. The green compact was made into a disc shape (diameter ~30 mm, t ~2.3 mm) by means of uniaxial pressing at 3.7 MPa. The specimens were heated under a 95% N_2/5% H_2 flowing atmosphere to 1450 °C in a horizontal tube furnace, where the reaction-bonding of Si occurred. In the post-sintering preparation process, the as-nitrided specimens (RBSN) were placed upon a BN-coated graphite crucible packed to full volume with BN–Si_3N_4 embedding powder. Post-sintering was carried out in a graphite resistance furnace at 1700–1900 °C for 2 h under a nitrogen atmosphere. The nitrogen pressure was 0.1 MPa for the sintering up to 1800 °C, while 0.9 MPa was employed for the sintering at 1900 °C. A reference SiC sample was fabricated by sintering at 1700 °C for 3 h in Ar using the mixing powders of SiC (~65 μm, purity >98%, Showa Denko, Tokyo, Japan), silicon, carbon and boron. A scanning electron microscope (SEM; JSM-6700F, JEOL, Tokyo, Japan) was used to observe the specimen surfaces and microstructures. The pore size distributions and specific pore area values were measured using a mercury porosimetry (Autopore IV 9510; Micromeritics, Norcross, GA, USA). The flow rate recorded as the input pressure was gradually increased using a porometer (CFP-1200-AEL; Porous Materials Inc., Ithaca, NY, USA).

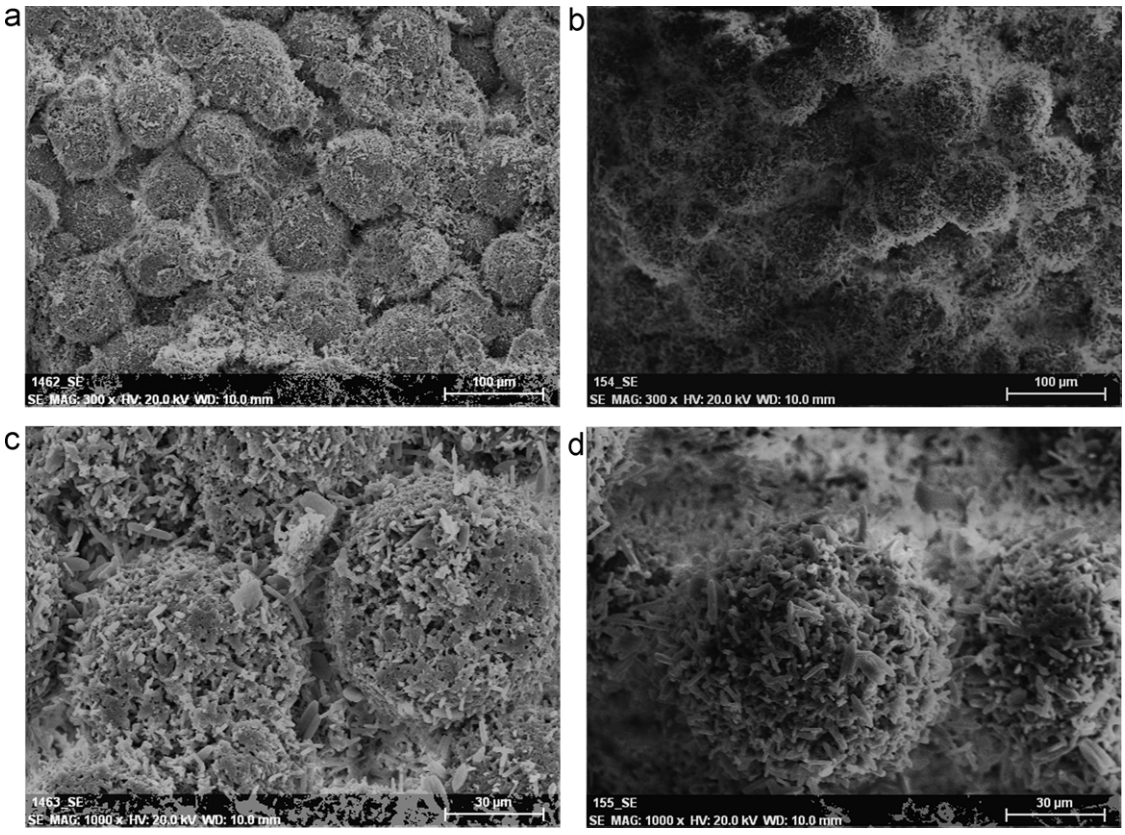

Fig. 3. Fracture surfaces of SRBSNs post-sintered at 1800 °C using m76.5 granules: (a) and (c) SRBSN-PG1 and (b) and (d) SRBSN-PG4.

3. Results and discussion

The compacting behavior of the presintered granules is plotted in Fig. 1. Non-classified granules (NCG) were sieved to produce four groups of mono-sized granules. They are classified according to the mean granule size. In the figure legends, the numbers following the character '*m*' represent the mean granule size in micrometers. The relationship of 'density *vs*. compacting pressure' was derived from 'load *vs*. displacement' data of a compression test of the granules. In the figure, the compacting pressure at the inflection point represents the fracture strength of the granules beyond which the green body undergoes substantial densification.[17] The strength of PG2 presintered at 1350 °C is higher than that of PG1 presintered at 1200 °C. While the strength of PG2 is independent of the granule size, that of PG1 increases as the granule size decreases. The strength of the m76.5 granule is about 2–3 MPa and 10 MPa for PG1 and PG2, respectively.

The nitridation rate of the reaction-bonded silicon nitride (RBSN) made from the m76.5 granule was 96.4% and 92.2% for PG1 and PG2, respectively. XRD analysis confirmed that no residual Si could be detected. The porosity of the RBSN was 57.4% and 61.6% for PG1 and PG2, respectively. The higher porosity of the RBSN made from PG2 is attributed to the higher sturdiness of the presintered granule and the lower nitridation rate.

Measurements of the porosity and the shrinkage of the SRBSNs are plotted in Fig. 2. A decrease in the porosity and an increase in the shrinkage were noted as the post-sintering temperature increased from 1700 °C to 1900 °C. The higher porosity of SRBSN-PG2 compared to that of SRBSN-PG1 is ascribed to the superior sturdiness of PG2 granules, which is analogous to the higher porosity in RBSN-PG2. Furthermore, considering the pore-former-free composition in the present research, it is notable that the porosity of the SRBSNs is more than 55% for SRBSN-PG2 and 45% for SRBSN-PG1. The porosity of SiC used as a reference was approximately 39%, which is similar to that of commercially used SiC filter.

The sturdiness of the spherical morphology of the granules in the SRBSNs is clearly observable on the fracture surfaces (Fig. 3). However, the contact configuration between the granules is substantially different depending on the strength of the presintered granule. Plane contact is dominant for SRBSN-PG1 (Fig. 3(a)), while point contact prevails for SRBSN-PG2 (Fig. 3(b)). The difference in the contact morphology can be understood by comparing the shaping pressure and strength of the presintered granules. The shaping pressure of 3.7 MPa is higher than that of the granule strength of m76.5-PG1 (about 2–3 MPa), while it is lower than that of the strength of m76.5-PG2 (about 10 MPa). It is interesting to note that the wide channels between granules are decorated by the intruding rod-like grains from the granule surface (Fig. 3(c) and (d)). The increased degree of interlocking by elongated grains between the granules leads to higher flexural strength of the current porous bodies.

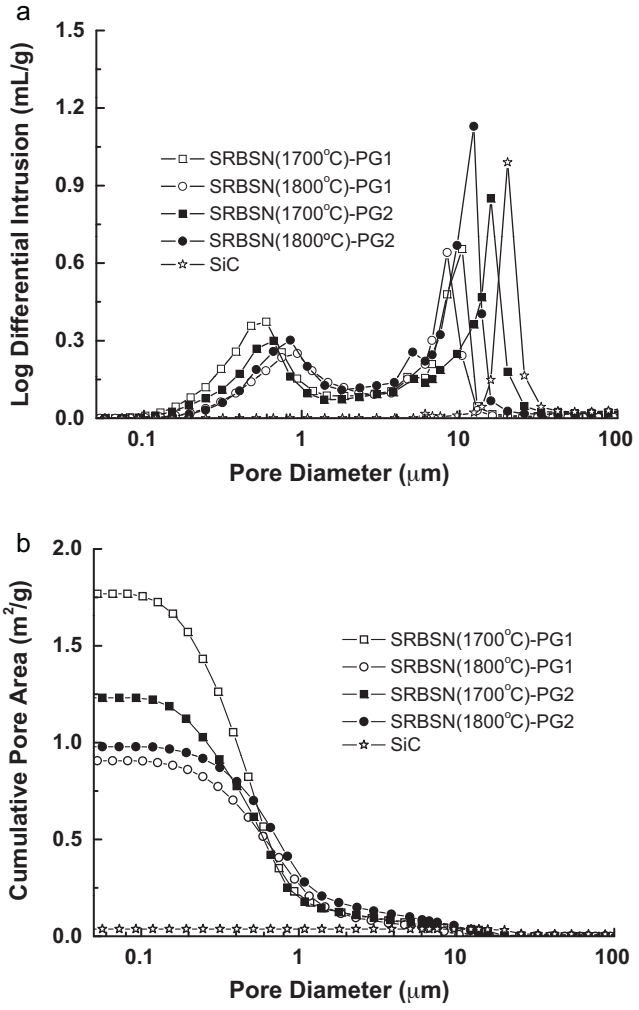

Fig. 4. Measurement of (a) the pore channel size and (b) the specific pore area. The SRBSNs were fabricated using m76.5 granules.

The distribution of the pore channel size and specific pore area of the SRBSNs were measured through mercury porosimetry. Fig. 4(a) reveals the dual-sized nature of the pore structure, consisting of both narrow channels ($d_p < 1\,\mu m$, 1st peak) and wide channels ($d_p \geq 10\,\mu m$, 2nd peak). The observation in Fig. 3, showing that the narrow channels form inside the granules, explains the similarity of the narrow channel size regardless of the granule size. The size of the wide channels decreases with the sintering temperature owing to the increased overall shrinkage. In contrast, the size of the narrow channels increases with the sintering temperature due to the coalescence of pores induced by the grain growth. This was possible because both the grain growth and the pore coalescence were restricted inside the granules due to the confinement of the liquid phase inside the granules by capillary forces. The channel size of the SiC is the highest (~20 μm) compared to that of the SRBSNs. The growth (coalescence) of the narrow channels as the sintering temperature increased resulted in a decreased pore area (Fig. 4(b)). It is remarkable to note that the specific pore area of the materials ranged from 0.91 to 1.77 m^2/g, which is more than 23–44 times the specific area of SiC (0.04 m^2/g). It is a well-known phenomenon that larger

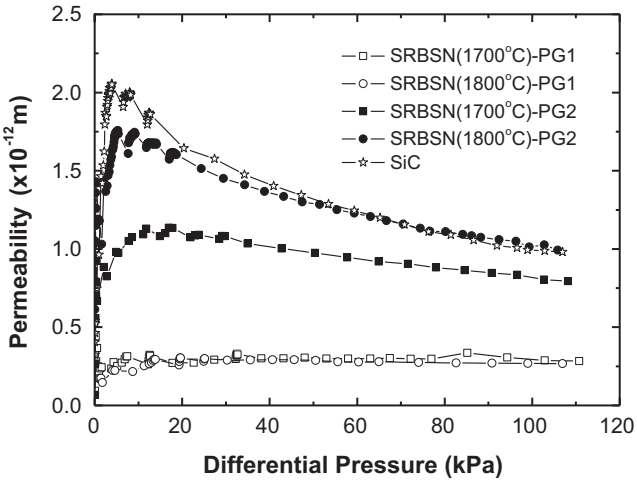

Fig. 5. Measurement of the permeability. The SRBSNs were fabricated using m76.5 granules.

particles are trapped in filters by an impact mechanism, while fine particles, because their movement is dominated by Brownian motion owing to their extremely small mass, are trapped by a diffusion mechanism.[18] Therefore, for nano-sized particulate matters, the filtration efficiency increases with the specific pore area.

The permeability (κ) is plotted as a function of the differential pressure in Fig. 5. Though the porosity of SRBSN(1800 °C)-PG2 is lower than that of SRBSN(1700 °C)-PG2, the permeability is higher due to the larger size of the wide pore channels. Finally, it should be emphasized that the permeability of SRBSN-PG2 fabricated at 1800 °C is comparable to that of reference SiC. The trade-off between the porosity and channel size resulted in nearly similar permeability between SRBSN(1800 °C)-PG2 and SiC.

4. Conclusions

In spite of the many strong points of the porous Si_3N_4 ceramics provided by their unique rod-like grains, their usage has been somewhat restricted owing to their low permeability. This study demonstrated that SRBSNs of comparable permeability to commercial SiC can be fabricated by granulation of the starting powders. Considering the higher specific pore area of the developed SRBSNs compared to that of SiC, superior filtration efficiency is expected for nano-sized PMs. Moreover, the formation of intragranular pores in addition to intergranular pores enables high porosity without the blending of fugitives. That is, SRBSNs using granules made of Si-additive mixture enable a low-carbon and green growth process.

Acknowledgement

This research project was supported by the Korea Institute of Materials Science, a branch of Korea Institute of Machinery and Materials.

References

1. Pastila P, Helanti V, Nikkila AP, Mantyla T. Environmental effects on microstructure and strength of SiC-based hot gas filters. *J Eur Ceram Soc* 2001;**21**(9):1261–8.
2. Laurila P, Mantyla T. Porous ceramics for hot gas cleaning; degradation mechanisms of SiC-based filters caused by long term water vapor exposure. *Ceram Trans* 2010;**210**:155–61.
3. Ohno, K., Shimato, K., Taoka, N., Santae, H., Ninomiya, T., Komori, T. and Salvat O, Characterization of SiC-DPF for passenger car. SAE technical paper series 2000; 2000-01-0185: 1–14.
4. Miwa, S., Abe, F., Hamanaka, T., Yamada, T. and Miyairi Y., Diesel particulate filters made of newly developed SiC. SAE technical paper series 2001; 2001-01-0192: 190–195.
5. Jayaseelan DD, Lee WE, Amutharani D, Zhang S, Yoshida K, Kita H. In situ formation of silicon carbide nanofibers on cordierite substrates. *J Am Ceram Soc* 2007;**90**(5):1603–6.
6. Shyam A, Lara-Curzio E, Watkins TR, Parten RJ. Mechanical characterization of diesel particulate filter substrates. *J Am Ceram Soc* 2008;**91**(6):1995–2001.
7. Kawai C, Yamakawa A. Effect of porosity and microstructure on the strength of Si_3N_4: designed microstructure for high strength, high thermal shock resistance, and facile machining. *J Am Ceram Soc* 1997;**80**(10):2705–8.
8. Kawai C, Matsuura T, Yamakawa A. Separation-permeation performance of porous Si_3N_4 ceramics composed of β-Si_3N_4 grains as membrane filters for microfilteration. *J Mater Sci* 1999;**34**: 893–6.
9. Yang JF, Zhang GJ, Ohji T. Fabrication of low-shrinkage, porous silicon nitride ceramics by addition of a small amount of carbon. *J Am Ceram Soc* 2001;**84**(7):1639–41.
10. Yang JF, Deng ZY, Ohji T. Fabrication and characterization of porous silicon nitride ceramics using Yb_2O_3 as sintering additive. *J Eur Ceram Soc* 2003;**23**:371–8.
11. Chen D, Zhang B, Zhuang H, Li W. Combustion synthesis of network silicon nitride porous ceramics. *Ceram Int* 2003;**29**:363–4.
12. Miyakawa N, Sato H, Maeno H, Takahashi H. Characteristics of reaction-bonded porous silicon nitride honeycomb for DPF substrate. *JSAE Rev* 2003;**24**:269–76.
13. Li W, Chen D, Zhang B, Zhuang H, Li W. Effect of rare-earth oxide additives on the morphology of combustion synthesized rod-like β-Si_3N_4 crystals. *Mater Lett* 2004;**58**:2322–5.
14. Park YJ, Choi E, Lim HW, Kim HD. Design of porosity level for porous Si_3N_4 ceramics manufactured by nitriding and post-sintering of Si powder compact. *Mater Sci Forum* 2007;**534**(536):1017–20.
15. Park YJ, Park BW, Lee JW, Yun HS, Song IH. Increase in the strength of Si-additive mixture granules by presintering. *Ceram Int* 2011;**37**(3): 1109–13.
16. Park, Y.J., Park. B.W., Lee. J.W., Yun. H.S. and Song, I.H., The characterization of porous sintered reaction-bonded silicon nitride ceramics fabricated by Si-additive mixture granules. Int J Appl Ceram Technol, in press, doi:10.1111/j.1744-7402.2011.02614.x.
17. Kondo Y, Hashizuka Y, Nakahara M, Yokota K. Granule properties in uniaxial press forming of alumina ceramics. *J Ceram Soc Jpn* 1995;**103**:1037–40.
18. Hinds WC. *Aerosol Technology*. 2nd ed. New York/Chichester/ Weinheim/Brisbane/Singapore/Toronto: John Wiley & Sons, Inc.; 1998.